Analysis of solitons in protoplanetary disc with MVS-1000M*

V.A. Vshivkov, A.V. Snytnikov

Abstract. With MVS-1000M the distribution of particle and gas density in the soliton were investigated, as well as their velocities, angular momentum, flow of gas and particles through soliton and vorticity of particle velocity. It is shown that in the soliton the high values of gas and dust densities and gas pressure arise. This fact probably explains the synthesis of organic compounds in protoplanetary disc.

1. Introduction

In recent times there is a great interest to the problem of organic matter genesis in the Solar System. In [1], the protoplanetary disc is considered as a catalytic chemical reactor for synthesis of primary organic compounds. The mean density and temperature in protoplanetary disc are very small. Because of this reason it is extremely important to find out how do the high values of temperature, pressure and density appear, that are necessary for chemical synthesis. The solitons that appeared in our computational experiments present one of the possible answers to this question.

2. Source equations

The dynamics of the dust component of protoplanetary disc is described by the Vlasov–Liouville kinetic equation. In the following, the dust particles will be called simply particles. To consider the motion of the gas component, the equations of gas dynamics are employed. The gravitational field is determined by the Poisson equation.

If we employ the collisionless approximation of the mean self-consistent field, then the Vlasov–Liouville kinetic equation is written down in the following form:

$$\frac{\partial f}{\partial t} + \vec{v}\nabla f + \vec{a}\frac{\partial f}{\partial \vec{v}} = 0,$$

where $f(t, \vec{r}, \vec{v})$ is the time-dependent one-particle distribution function along coordinates and velocities, $\vec{a} = -\nabla\Phi + \frac{\vec{F}_{\text{fr}}}{m}$ is the acceleration of unit mass

---

particle, $\vec{F}_{\text{fr}}$ is the friction force between the gas and the dust components of the medium. Gravitational potential Φ could be divided into two parts:

$$\Phi = \Phi_1 + \Phi_2,$$

where Φ_1 presents either the potential of immobile central mass (either galactic black hole or protostar) or the potential of a rigid system which is out of disc plane (either the stars of galactic halo or molecular cloud). The second part of the potential Φ_2 is determined by the additive distribution of the moving particles and gas. Φ_2 satisfies the Poisson equation

$$\Delta\Phi_2 = 4\pi G \Sigma \rho.$$

In the case of infinitesimally thin disc, the bulk density of the mobile media $\Sigma\rho = \rho_{\text{part}} + \rho_{\text{gas}}$ is equal to zero (ρ_{part} is the particle density, ρ_{gas} is the gas density). At the disc with the surface density σ there is a shear of the normal derivative of potential. This shear gives a boundary condition for the normal derivative of the potential Φ_2:

$$\frac{\partial \Phi_2}{\partial z} = 2\pi G \sigma.$$

The equations of gas dynamics take the following form:

$$\frac{\partial \rho}{\partial t} + \nabla(\rho\vec{v}) = 0, \qquad \rho\Big[\frac{\partial \vec{v}}{\partial t} + (\vec{v}\nabla)\vec{v}\Big] = -\nabla p + \vec{F},$$

$$\frac{\partial E}{\partial t} + (\vec{v}\nabla)E = -\nabla(p\vec{v}) + Q + (\vec{F}, \vec{v}) - \nabla W,$$

where $E = \big(\varepsilon + \frac{v^2}{2}\big)$ is the density of gas full energy, $\varepsilon = \varepsilon(\rho, T)$ is the internal energy of gas, $p = p(\rho, T)$ is the pressure of gas, $\vec{W} = \nabla T$ is the heat flow, Q is the increase of energy due to chemical reactions and radiation. $\vec{F}$ is the external force which is defined by the following expression:

$$\vec{F} = \rho\nabla\Phi - k_{\text{fr}}(\vec{u} - \vec{v}).$$

Here k_{fr} is the coefficient of friction between gas and dust components of the disc, $\vec{u}$ is the dust velocity, $\vec{v}$ is the gas velocity. In the case of the flat disc (so called 3D2V model), the form of equation remains the same with the only exclusion: the bulk density ρ is replaced with the surface density σ. In this paper, we shall consider only the flat disc model.

In the full description of the protoplanetary disc, these equations are complemented with the equations for chemical reactions in gas phase and the equations for simulation of coagulation processes in the dust component.

The following quantities were chosen as basic characteristic parameters for transition to sizeless variables:

- distance from the Sun to the Earth $R_0 = 1.5 \cdot 10^{11}$ m;
- mass of the Sun $M_\odot = 2 \cdot 10^{30}$ kg;
- gravitational constant $G = 6.672 \cdot 10^{-11} \ \cdot \text{m}^2/\text{kg}^2$.

Corresponding characteristic values of the particle velocity (V_0), potential (Φ_0), time (t_0), and surface density (σ_0) are written down as

$$V_0 = \sqrt{\frac{GM_\odot}{R_0}} = 30 \text{ km/s}, \qquad \Phi_0 = V_0^2 = \frac{GM_\odot}{R_0},$$

$$t_0 = \frac{R_0}{V_0} = 5 \cdot 10^6 \text{ s} = \frac{1}{6} \text{ year}, \qquad \sigma_0 = \frac{M_\odot}{R_0^2}.$$

Further, all the parameters are given in sizeless units.

The Vlasov–Liouville equation is solved by Particles-in-Cells method [2]. To solve the equations of gas dynamics Fluids-in-Cells method is employed [3].

In the authors' opinion, an efficient Poisson equation solver could be built only if the peculiarities of the problem were taken into account. These peculiarities are the following. First, the problem is non-stationary. Second, at initial moment of time the disc has axial symmetry. And third, all the matter is situated in the disc plain. Having considered all these peculiarities, a special Poisson equation solver was built on the basis of the fast Fourier transform [4].

The implemented methods for solution of the Vlasov equation and gas dynamics equations are described in more detail in [5]. Parallelization scheme is presented in [6].

Initial distribution of the particle and gas density is set according to the model of solid body rotation:

$$\sigma(r, \varphi) = \begin{cases} \sigma_c \sqrt{1 - \left(\frac{r}{r_0}\right)^2}, & r < r_0, \\ 0, & r \geq r_0, \end{cases}$$

where r_0 is the radius of the corresponding disc. The coefficient σ_c is chosen for the total mass to be equal to the given (M):

$$M = 2\pi \int_0^{r_0} \sigma r \, dr = 2\pi\sigma_c \int_0^{r_0} \sqrt{1 - \left(\frac{r}{r_0}\right)^2} r \, dr = \frac{2\pi}{3}\sigma_c r_0^2,$$

then

$$\sigma_c = \frac{3M}{2\pi r_0^2}.$$

Initially for radial component of the particles' velocities a normal distribution is set:

$$f_v = \frac{1}{\sqrt{2\pi}T_D}\exp\left(-\frac{v_R^2}{2T_D^2}\right).$$

Here T_D is the dynamic temperature of particles. An additional parameter is the pressure of gas in the disc center.

3. Parameters of computational experiments

Table 1. Technical parameters of experiments on 8 processors

Grid size $N_R \times N_\varphi \times N_Z$	Number of particles	Computation time, hours
$120 \times 128 \times 128$	10^6	8
$200 \times 256 \times 128$	$25 \cdot 10^6$	30
$300 \times 256 \times 128$	$50 \cdot 10^6$	49

The technical parameters of computational experiments are given in Table 1. The physical parameters that are set as initial data for the computational experiment are given below. The most important among them are the masses: the mass of central body $M_\odot$, the mass of gas component M_G, and the mass of dust component M_P:

Radius of dust disc, R_P 1.0
Radius of gas disc, R_G 1.0
Mass of dust component, M_P 1.0
Mass of gas component, M_G 1.0
Mass of central body, $M_\odot$ 0.5
Dynamic temperature of dust particles, T_D 1.0
coefficient of friction, k_{fr} 1.0
Gas pressure in the center, p_0 .... 0.001

In the course of computational experiments, it was found out that the solitons definitely arise when the mass ratio is $M_P : M_G : M_\odot = 2 : 2 : 1$. Also, soliton formation is affected by the coefficient of friction between dust and gas components. When this coefficient substantially decreases the solitons do not arise. The increase of the radius of either gas or dust component affects the system like the decrease of the corresponding mass and makes the disc more unstable. The dynamic temperature of dust particles and gas pressure in the disc center make the corresponding component of the disc more stable. Nevertheless, the influence of these quantities on the soliton formation is a question of further studies.

Generally about 40 soliton simulation experiments were conducted with MVS-1000M. Six computational experiments of this array are presented in this paper. The physical parameters were identical in all experiments, but the number of particles and grid size were different. From Table 1 it follows that such experiments require large computational resources. To compute dust and gas motion even with a small grid it is necessary to employ 8 processors. The computational experiments on finer grids were conducted with

Table 2. Computational experiments

Experiment	Grid size	Number of particles	Size of region under study	Center of region under study
I	$120 \times 128 \times 128$	10^6	2.0×2.0	$(0.0, 0.0)$
II	$200 \times 256 \times 128$	$25 \cdot 10^6$	2.0×2.0	$(0.0, 0.0)$
III	$200 \times 256 \times 128$	$25 \cdot 10^6$	0.3×0.3	$(0.6, 0.6)$
IV	$200 \times 256 \times 128$	$25 \cdot 10^6$	0.4×0.4	$(-0.71, 0.1)$
V	$300 \times 256 \times 128$	$50 \cdot 10^6$	3.0×3.0	$(0.0, 0.0)$
VI	$300 \times 256 \times 128$	$50 \cdot 10^6$	1.0×1.0	$(-0.5, -0.5)$

the so called "checkpoints". A checkpoint means that all the data of the program are saved to a file, one file for each processor, and then the program stops. After a while, the computational experiment is continued starting from the saved data.

The difference between the computational experiments are shown in Table 2. The computations are conducted with the grid in cylindrical coordinate system. Nevertheless, to draw a 2D spatial distribution of some function $h(r, \varphi)$ a Carthesian grid is employed. This Carthesian grid is introduced in the same domain and the distribution—now $h(x, y)$ is computed on this grid directly with particles.

Moreover, a small region of the disc is selected for detailed study, and in this region the distribution $h(x, y)$ is drawn with a Cartesian grid of the same size as in the whole disc. The same way a telescope shows some part of the sky in more detail.

In the computational experiments with the same grid size and the same number of particles, different regions of the disc were considered. From both the physical and the computational point of view it is the same experiment. Nevertheless, it is necessary to conduct a number of experiments with the same parameters due to the following reasons. First, it is impossible to draw the distribution in the whole disc in great detail. Second, it becomes clear which region of the disc is worth studying in detail only when the experiment is over. It should be noted that there is no loss of precision, since the distribution in a small part of the disc is also computed with particles.

The pictures in Section 6 are an exclusion from this rule. They present distributions from the vicinity of the soliton, that is, in a region of a very small size (less than 0.2×0.2). They are obtained by cutting the corresponding part of the grid from the distribution in a large region.

Both in the whole disc and in small size regions the distribution is drawn by the same rules: the white color corresponds to maximal value, the black color—to zero, the scale is logarithmic.

4. Grid influence on the computational experiments

Computational experiments with the same physical parameters were conducted on the following sequence of grids: $120 \times 128 \times 128$, $200 \times 256 \times 128$, and $300 \times 256 \times 128$ nodes. The resulting distributions of particle density are shown in Figure 1.

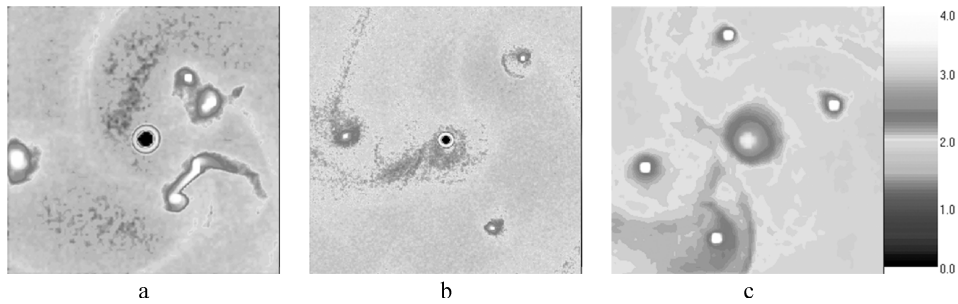Density waves that arise on the coarse grid ($120 \times 128 \times 128$ nodes) are different from solitons in that they have large size, as it is seen in Figure 1a

Figure 1. Density waves on different grids: a) Experiment I, b) Experiment II, c) Experiment V
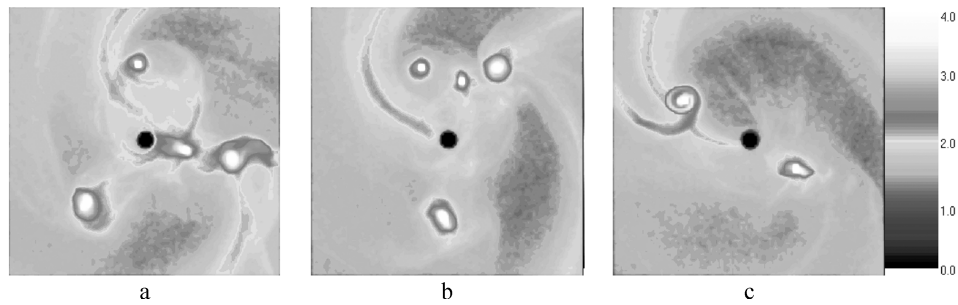
Figure 2. Decay of density waves on the coarse grid in Experiment I: a) particle density distribution at the time 4.4, b) at 4.8, and c) at 5.2
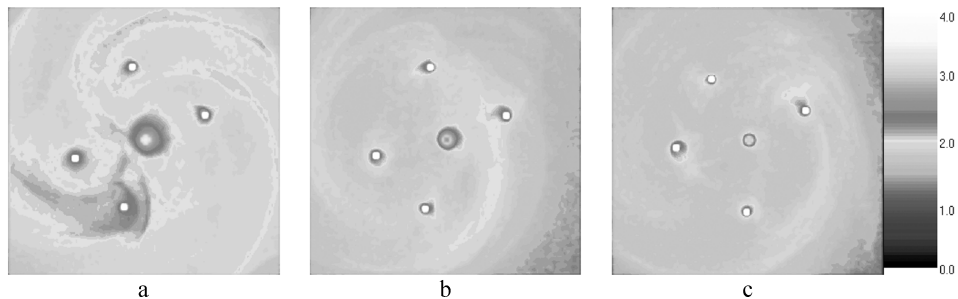
Figure 3. The stability of density waves on the fine grid in Experiment V: a) particle density distribution at the time 4.0, b) at 6.0, and c) at 8.0

in comparison with Figures 1b and 1c. Another difference is that they are unstable. These density waves decay in a short period of time $\Delta T = 0.4$ (Figure 2).

On the contrary, on finer grids density waves have small size (Figure 3) and they remain stable during a large period of time $\Delta T = 4.0$. In Figure 3c it is seen that upper and lower solitons are shifted from initial position. But the most important result is that these density waves remain stable and keep small size. The solitons on fine grid are particularly considered in Section 6.

5. Soliton behavior

Soliton is an lone density wave. On the fine grid (Experiment V) the solitons were nearly immobile during a short period of time. Considered particle density distribution in dynamics it is clearly seen. In Figure 4, this distribution is shown in the three successive moments of time. The difference in time between them is 0.2. The four solitons do not shift during this short period, though the density distribution in the whole disc changes significantly.
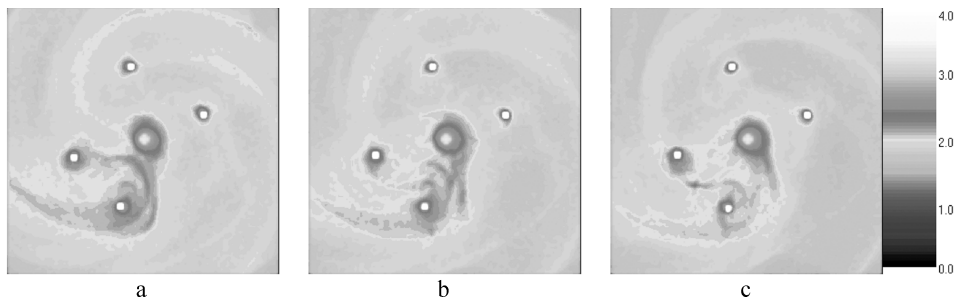

Figure 4. The immobile solitons on the fine grid in Experiment V:
a) particle density distribution at the time 4.0, b) at 4.2, and c) at 4.4

The following fact proves that these structures are density waves and not clumps of dust. The matter of the disc rotates around the disc center, but the solitons remain in its position. It should be noted that in fact the soliton moves as a density wave, but its velocity could be oriented either along the flow or in the opposite direction.

So the soliton forms a small region of high density in the flow. It is similar to a magnetic lens that focusses a beam of charged particles. The difference is that the focussing field in the case of soliton is created by the beam itself.

Let us consider the soliton scaled-up. With the same physical parameters the soliton either remained nearly immobile (Experiment III, Figure 5) or oscillated around some point (Experiment IV, Figure 6). Let us remind that these are two different solitons from the same computational experiment.
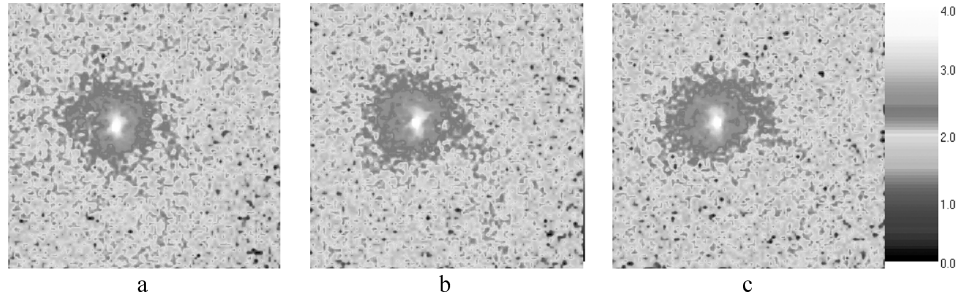
Figure 5. The immobile soliton scaled-up in Experiment III:
a) particle density distribution at the time 4.01, b) at 4.05, and c) at 4.09
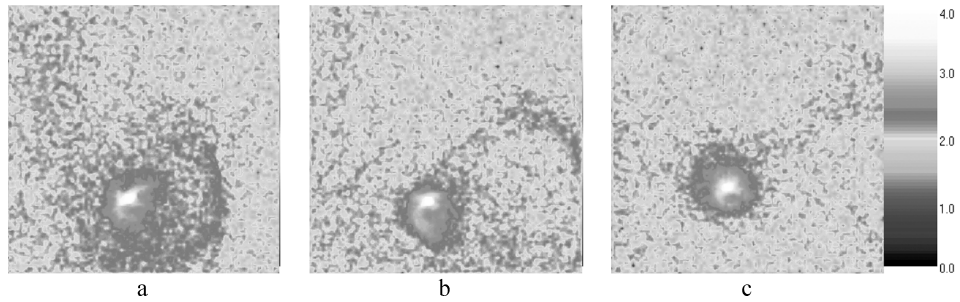

Figure 6. The oscillating soliton scaled-up in Experiment IV:
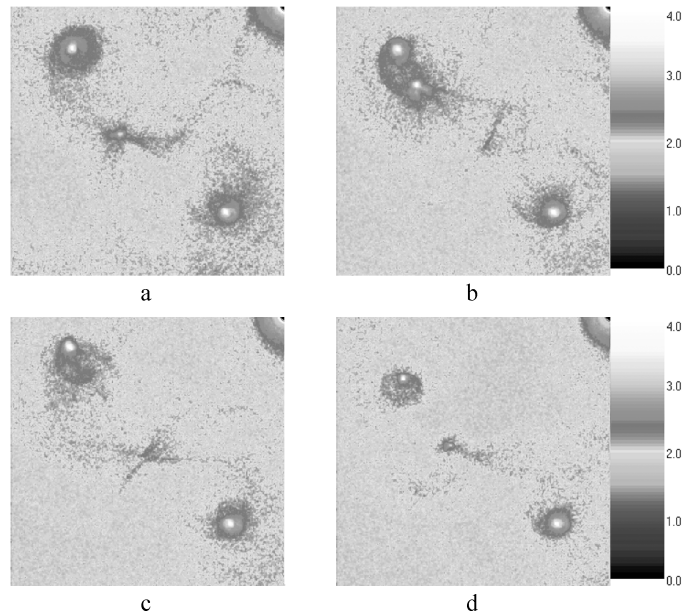a) particle density distribution at the time 4.01, b) at 4.09, and c) at 4.17

Figure 7. Absorbtion of a density wave by the soliton in Experiment VI:
a) particle density distribution at the time 4.76, b) at 4.96, c) at 5.04,
and d) at 5.2

In Experiment VI, the absorption of a density wave by soliton occurred, Figure 7. First the density wave arises (see Figure 7a), then it approaches the soliton (see Figure 7b). After absorption, the soliton deviates from the initial position (see Figure 7c) but then returns back (see Figure 7d). It should be noted that such a phenomenon is impossible for clumps. Thus Figure 7 proves wave nature of the structures observed in our computational experiments — the solitons.

6. Soliton structure

For a particular study of the soliton let us consider the main physical quantities in its vicinity:

- Particle density distribution σ_P;

- Vorticity of particle velocity $\nabla \times \vec{v}$;

- Distribution of particle velocity in the horizontal and vertical sections of the soliton, $v_x(y)$ and $v_y(x)$;

- Distribution of particle flow in the horizontal and vertical sections of the soliton, $\sigma_P v_x(y)$ and $\sigma_P v_y(x)$;

- Gas density distribution σ_G.

Experiment V is considered now. Soliton vicinity is the region, where particle density is more than 10 times higher than mean particle density in the disc. The vicinity is cut from the distribution computed for the region with the size 1.0×1.0, its center in $(-0.5, -0.5)$. Cutting is performed along the nodes of Carthesian grid that is used to draw the distribution in the large region. This approach enables to consider that an arbitrary region of the disc though the precision is less than in Section 5. All the quantities are given for the moment of time 6.0.

Figure 8a shows the central region of the disc with the size 3.0×3.0. The considered soliton is pointed by the arrow. Figure 8b shows the vicinity of
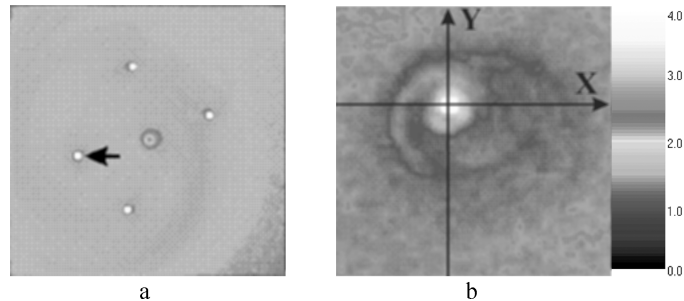

Figure 8. Particle density distribution in the soliton in Experiment V

the soliton. The size of the region in Figure 8b is 0.2×0.2, its center is the point $(-0.77, -0.15)$.

In Figure 8, it is seen that the size of region with high density (soliton kernel) is very small. Moreover, the white color of the kernel shows that particle density is by several orders of magnitude greater than in the surrounding region. Let us consider the 1D density plots to obtain the quantitative data. The axes X and Y go through soliton kernel, that is, through the point $(-0.78, -0.17)$, as it is shown in Figure 8b.

Figure 9 show that particle density in the soliton kernel is by six orders of magnitude greater than in the surrounding region. The width of peak is equal to 0.01.

Now let us consider particle velocity field in the vicinity of soliton. Figure 10a shows vertical velocity of particles in the horizontal section of the soliton and Figure 10b — horizontal velocity of particles in the vertical section of the soliton. Thus the normal component of velocity is displayed.

It could be noticed that particle velocity is close to zero in the center and on the edge of the soliton. On the contrary, velocity has its extremum at the distance of about half the soliton radius from the center of soliton.

Vorticity distribution for particle velocity vector (Figure 11) is a matter of special interest. In Figure 11, black means counter-clockwise rotation, and white means the clockwise rotation. Soliton kernel is surrounded by an open black circuit. Zero of velocity in Figure 10 is shifted from the maximum of density in Figure 9. All these facts enable to state that the soliton rotates around the point which is close to the kernel, but not in the kernel itself!
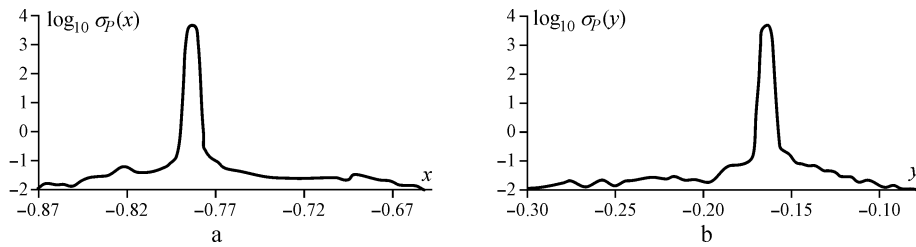

Figure 9. Particle density in a) the horizontal and b) the vertical cross sections of the soliton
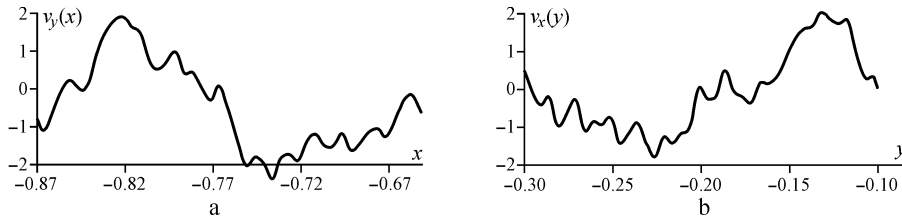

Figure 10. Particle velocity in a) the horizontal and b) the vertical cross sections of the soliton
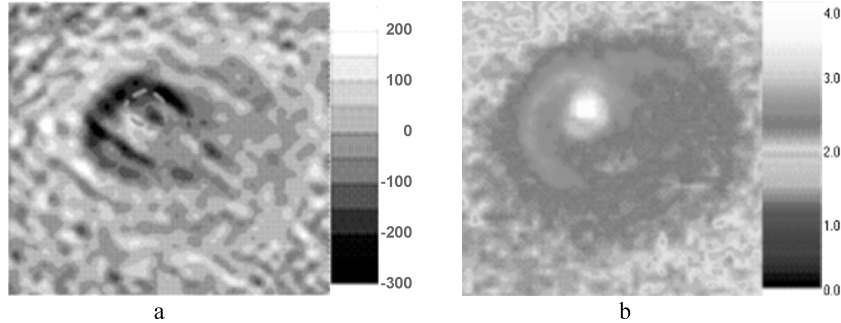
Figure 11. The distribution of a) the vorticity for particle velocity in the vicinity of the soliton $\nabla \times \vec{v}(x, y)$ and b) the particle density. The size of the region is 0.2×0.2, its center is the point $(-0.77, -0.15)$
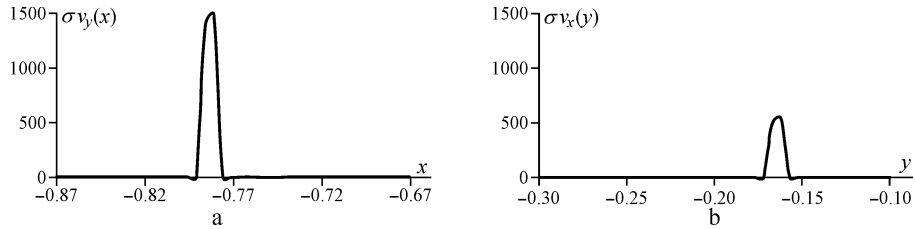

Figure 12. Particle flow through a) the horizontal and b) the vertical cross sections of the soliton
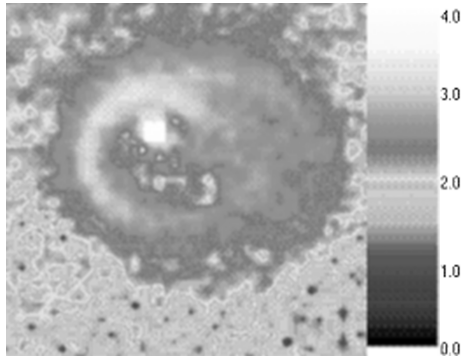

Figure 13. Absolute value of particle flow in the vicinity of the soliton, $|\sigma v_x(y)|$. The size of the region is 0.2×0.2, its center is the point $(-0.77, -0.15)$

Moreover, Figure 10 confirms that the soliton really remains almost immobile, because particle velocity in the center is close to zero. Once more let us take into account that velocity of the soliton as a wave is equal to flow velocity but has the opposite direction in this case.

The matter flow through the region of soliton is of great interest. From the distribution of absolute value of velocity is is seen that particles accelerate when going through soliton region. The disc as a whole rotates counter-clockwise, but the vector of the matter flow through soliton is oriented in the opposite direction. Also the extremum of the flow in Figure 12 is shifted from the maximum of density in Figure 9 to the distance of about half the size of soliton kernel.
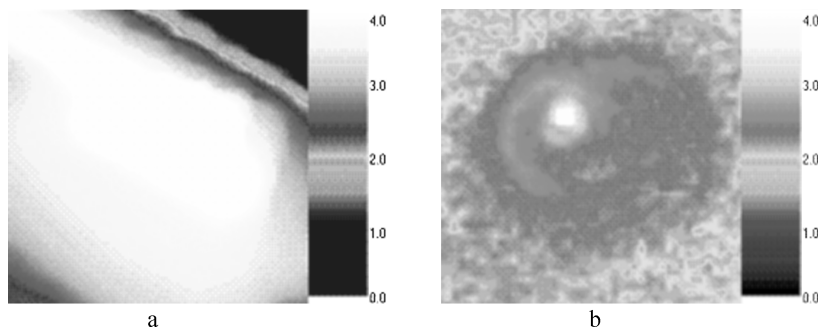
a   b

Figure 14. The distribution of a) gas density in the vicinity of the soliton $\sigma_G(x, y)$ and b) the particle density. The size of the region is 0.2×0.2, its center is the point $(-0.77, -0.15)$

The most important result of these computational experiments is shown in Figure 14. Since chemical reactions take place mostly in gas phase, with the dust particles acting only as a catalyst, it is extremely important to know the behavior of gas in the vicinity of soliton. In Figure 14 gas density distribution is compared to particle density distribution in the vicinity of soliton.

Figure 14 shows that the density of gas and, consequently, its pressure is also by several orders of magnitude higher than in the surrounding disc. The region with high density of gas is much larger than soliton kernel. The reason, probably, is that because of its pressure gas cannot form dense structures of small size.

7. Conclusion

High densities and pressures of gas may arise in soliton region as it is shown in the computational experiments. These conditions probably make the catalytic synthesis of primary organic compounds possible.

It means that MVS-1000M enables to obtain physical results on simulation of the evolution of protoplanetary disc. To the present moment an evidence is obtained that sufficient conditions for organic synthesis may arise in protoplanetary disc.

Further work will include the extension of the program with chemical kinetics equations and with the equations for coagulation of dust particles. It is supposed that the solution of these equations could be easily parallelized since coagulation and chemical synthesis processes are considered within one cell. In this case, the importance of MVS-1000M will increase since these equations will give a great computational workload.

References

[1] Snytnikov V.N., Dudnikova G.I., Gleaves J.T., et al. Space chemical reactor of protoplanetary disk // Adv. Space Res. — 2002. — Vol. 30, No. 6. — P. 1461–1467.

[2] Grigoryev Yu.N., Vshivkov V.A., Fedoruk M.P. Numerical "Particle-in-Cell" Methods. Theory and Applications. — Utrecht: VSP, 2002.

[3] Belotserkovsky O.M., Davydov Yu.M. Fluids-in-Cells Method in Gas Dynamics. — Moscow: Nauka, 1982 (In Russian).

[4] Snytnikov A.V. A parallel program for simulation of disc-shaped self-gravitating systems // NCC Bulletin. Series Comp. Science. — Novosibirsk: NCC Publisher, 2003. — Iss. 19. — P. 73–81.

[5] Snytnikov V.N., Vshivkov V.A., Dudnikova G.I., et al. Numerical simulation of N-body gravitational systems with gas // Vychislitel'nye Tehnologii. — 2002. — Vol. 7, No. 3. — P. 72–84.

[6] Kuksheva E.A., Malyshkin V.E., Nikitin S.A., et al. Numerical simulation of self-organization in gravitationally unstable media on supercomputers // PaCT-2003. — 2003. — P. 354–368. — (Lect. Notes Comput. Sci.; 2763).